Many-particle effects and nonlinear optical properties of GaAs/(Al,Ga)As multiple-quantum-well structures under quasistationary excitation conditions

K.-H. Schlaad and Ch. Weber
Fachbereich Physik der Universität Kaiserslautern, Federal Republic of Germany

J. Cunningham
AT&T Bell Laboratories, Holmdel, New Jersey 07733-1988

C. V. Hoof and G. Borghs
Interuniversitair Micro Electronica Centrum, Leuven, Belgium

G. Weimann
W. Schottky Institute, München, Federal Republic of Germany

W. Schlapp and H. Nickel
Forschungsinstitut der Deutschen Bundespost, Darmstadt, Federal Republic of Germany

C. Klingshirn
Fachbereich Physik der Universität Kaiserslautern, Federal Republic of Germany
(Received 17 July 1990)

Quasi-two-dimensional (2D) carrier systems of GaAs/(Al,Ga)As multiple-quantum-well structures are studied under quasistationary excitation conditions using the pump and probe beam and the luminescence spectroscopy. In the low- to medium-density regime the saturation of the $n_z=1$ exciton resonances dominates the nonlinear optical propeties. The low-temperature saturation density is found to be $N_s \approx 4\times 10^{16}$ cm^{-3}, independent of the well width L_z. The carrier-induced energetic shift of the 1hh-exciton resonance as a function of L_z shows the dimensional dependence of the screening properties of the carriers. The 2D limit is reached at well widths smaller than 50 Å, whereas the 3D behavior occurs already at $L_z=190$ Å. In the high-excitation regime, the renormalization of the fundamental band gap is investigated as a function of the electron-hole plasma density. The density and the reduced band gap are determined via systematic evaluations of both gain and luminescence spectra. The observed behavior can be described by a strict 2D theory using effective exciton parameters in order to account for the finite well widths of the structures. The same theory describes very well an n-type modulation-doped quantum well if an independent shift of each subband—according only to its specific carrier density—is assumed. The correlation enhancement of the band-to-band transitions was observed in an n-type modulation-doped sample where all excitonic features were quenched by the doping density. The study of the higher subbands reveals that both exciton bleaching and subband renormalization are due mainly to a direct occupation of the specific subband; we find that the intersubband effects via Coulomb screening are negligible.

I. INTRODUCTION

The progress in manufacturing high-quality layered semiconductor structures since the beginning of the eighties led to a strong increase in research activities on their optical properties and use as new electronic devices of the so-called (multiple-) quantum-well structures (MQWS). For recent reviews, see, e.g., Refs. 1–3.

This contribution reviews the recent activities of our research group concerning the nonlinear optical properties of GaAs/(Al,Ga)As MQWS under the illumination with nanosecond laser pulses. This stands for the realization of quasistationary excitation conditions: the duration of the exciting light pulse is long in comparison with the intrinsic time constants of the semiconductor material.

The observed phenomena can be divided into two parts which both depend on the number of optically created carriers.

(i) The low- to medium-density domain is dominated by excitonic features; we studied the bleaching and the shift of the quasi-two-dimensional (2D) excitons as a function of the electron-hole pair density.

(ii) The presence of an electron-hole (e-h) plasma is responsible for the high-density features of the samples; band-gap renormalization and correlation effects are investigated in this case.

II. EXPERIMENTAL SETUP

For our investigations several molecular-beam-epitaxy-(MBE-) grown samples on GaAs substrates were avail-

able. We studied undoped MQWS with different well widths L_z between 36 and 190 Å and an n-type modulation-doped MQWS (MDQW) with $L_z = 147$ Å and $N_D = 2.8 \times 10^{11}$ cm^{-2}. The carriers were created optically with pulsed-excimer-laser-pumped dye-laser systems. The pulse duration was about 10 ns and we reached power densities up to 10 MW/cm^2. We generated the carriers directly in the wells above the fundamental band gap with photon energies around 1.7 eV. Lattice temperatures between 5 and 77 K were realized.

In order to prepare the samples for transmission experiments the substrate was removed by a selective etching technique.[4] Optionally one surface of the samples was covered with an antireflection coating. The photoluminescence was detected in transmission as well as in reflection. The reason why we did not find any remarkable difference between both techniques lies in the small sample thickness. To achieve absorption spectra we used a common pump- and probe-beam setup. Transmission and luminescence signals were detected simultaneously by using an optical multichannel analyzer behind a spectrometer.

III. THE LOW- TO MEDIUM-DENSITY REGIME: EXCITONIC FEATURES

All considerations in this chapter use a linear relation between the reduction of the excitonic oscillator strength f and the density N of e-h pairs, with the condition that N is small (i.e., Na_{2D}^2 is of the order of unity, with a_{2D}, the excitonic Bohr radius)[5,6]

$$\frac{\delta f}{f_{1s}} = -\frac{N}{N_s} . \tag{1}$$

Herein N_s denotes the saturation density of the excitonic resonance, which is defined as a decrease of the oscillator strength by a factor of 2. Furthermore, we assume a linear dependence between the reduction of the oscillator strength and of the peak value of the absorption of the excitonic structure $\delta\alpha$, thus neglecting effects due to the collision broadening[5,7,8]

$$\frac{\delta f}{f_{1s}} \simeq \frac{\delta\alpha}{\alpha_{1s}} \propto N . \tag{2}$$

Assuming a complete occupation of the states with excitons, we use the following theoretical expression for the saturation density:[5]

$$N_s = \frac{0.117}{\pi a_{2D}^2} . \tag{3}$$

For the interpretation of the carrier-density-induced blue shift δE of the lowest exciton (1hh-x) we made use of the relationship[9]

$$\frac{\delta E}{E_{1s}} = C\frac{\delta f}{f_{1s}} . \tag{4}$$

The shift coefficient C is zero for 3D carrier systems, which has been proven experimentally.[10–12] Theoretical considerations for a 2D exciton gas at $T = 0$ K (Ref. 13) give the shift of

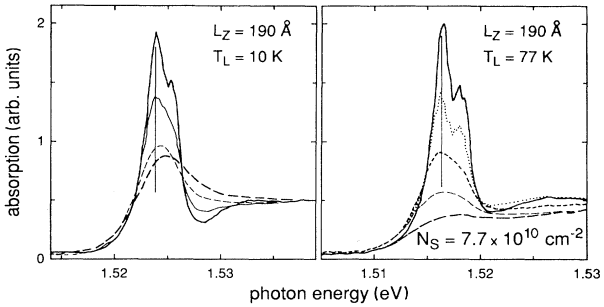

FIG. 1. Saturation of the 1hh-x at $T_L = 10$ K (left) and $T_L = 77$ K (right) of a 190-Å MQWS.

$$\frac{\delta E}{E_{1s}} \simeq 3.86\pi a_{2D}^2 N. \tag{5}$$

The numerical value of C is 0.5 in this case. To determine the magnitude of $\delta\alpha$ and δE, Gaussian or Lorentzian fitting curves were used.

Taking the numerical values for the excitonic saturation density from literature one gets different results—depending on the experimental techniques used. The values of one-beam experiments at room temperature are about $(3-5)\times 10^{11}$ cm^{-2} (Refs. 9, 10, and 14) while the investigation of n-type MDQW samples show that a doping density in the range of $(1-3)\times 10^{11}$ cm^{-2} is high enough to bleach the structure of the first electron–heavy-hole exciton (1hh-x).[15]

The evaluation of our gain spectra gives a band-gap shift of already -21 meV for a 130-Å sample at helium temperature under an e-h plasma density of 3×10^{11} cm^{-2} while the excitonic rydberg Ry_{2D}^* is only about 8 meV at zero density; with increasing carrier density the exciton energy is nearly constant in 3D and shifts even slightly blue in quasi-two-dimensional systems. So we have to look for much lower values for the saturation density N_s than those mentioned above.

Figure 1 shows results of a two-beam experiment. We investigated the 1hh-x bleaching of a 190-Å MQWS at lattice temperatures T_L of 10 K (left) and 77 K (right), respectively. The carriers were created optically. In order to achieve low carrier temperatures in the first case ($T_L = 10$ K) the excitation energy was chosen to 1.54 eV. To deduce the carrier density from the spectra we used formula (1) to extrapolate the well-known values of the plasma regime (the evaluation of the plasma spectra is described in the next paragraph).

At 77 K we observe a decrease of the absorption height of the 1hh-x resonance with increasing pump power due to population effects while the spectral position of the exciton is still unchanged. This behavior is different from the case of low lattice temperatures (left side of Fig. 1). Here we find a blue-shifted maximum at the highest excitation intensities in the spectra, which is due to exchange interactions in the exciton gas. This shift only occurs if the condition $k_B T/E_{1s} \ll 1$ is fulfilled and vanishes with increasing temperature T.[5] We ascribe the effects at 77 K to the correlation enhancement of the continuum states; an evaluation of the created density is not possible

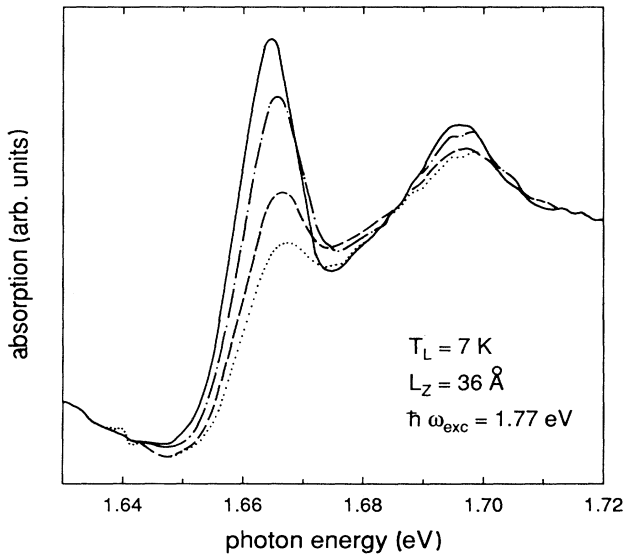

FIG. 2. Population-induced blue shift of the 1hh-x resonance of a 36-Å MQWS.

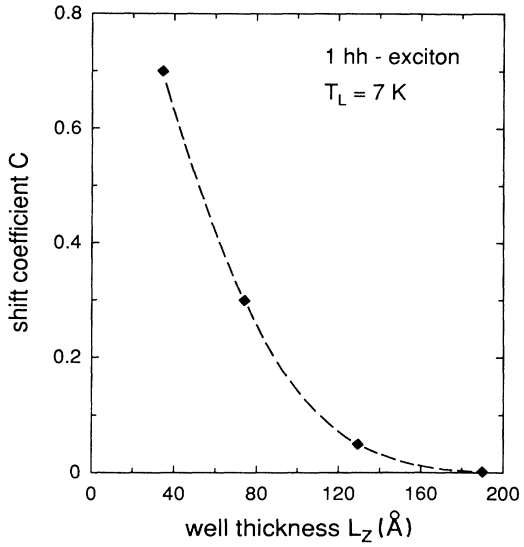

FIG. 4. Dependence of the shift coefficient C on the well width L_z.

in this case.

The results of the fit procedure are $N_s = 7.7 \times 10^{10}$ cm^{-2} for the 190-Å MQW (multiple quantum well) at 77 K and $N_s = 5 \times 10^{10}$ cm^{-2} for a 130-Å sample at 6 K. The theoretical value of Eq. (3) gives $N_s = 7.6 \times 10^{10}$ cm^{-2} using the exact 2D Bohr radius a_{2D} of 70 nm. Replacing a_{2D} by the effective Bohr radius of a quasi-two-dimensional system (which is about 130 Å for the 130-Å MQW) we get $N_s = 2.2 \times 10^{10}$ cm^{-2}. The difference of both experiment and theory is small in consideration of the numerous assumptions which have been made.

As mentioned above there is no shift of the spectral position of the exciton in 3D. This behavior is due to the compensation of two effects: On the one hand, population effects result in an energetic red shift of the band gap while on the other hand the excitonic binding energy is reduced.[16,17]

It was one of our aims to study the continuous transition from a 2D to a 3D carrier system. Therefore we investigated samples with well widths L_z of 36, 75, 130, and 190 Å. The 3D behavior is just reached in the 190-Å sample and is emphasized by vertical lines in Fig. 1. Figure 2 shows the 1hh-x absorption spectra of a 36-Å MQW under different excitation conditions. The expected excitonic blue shift is clearly recognizable in this case.

In order to evaluate the experimental data, the energetic shift δE of the exciton is drawn in Fig. 3 as a function of the reduced oscillator strength δf for different samples and lattice temperatures. The shift coefficient C of Eq. (4) is determined from the slope of the resulting straight line.

Theoretical predictions[18] give a resulting red shift of the exciton for temperatures above 50 K and therefore a negative C. Studying the 75-Å sample we find a reduction of C from 0.3 to 0.1 by raising the temperature from 7 to 77 K.

The relation between L_z and C is demonstrated for the $T_L = 7$ K data in Fig. 4. We give an interpretation of this behavior as follows: the 2D limit is characterized by a reduced screening of the Coulomb interaction of the carriers compared to the 3D system. This results in an enhanced influence of the exchange interaction and leads finally to the observed blue shift of the excitonic resonance. With increasing L_z the screening of carriers becomes more and more important; the 3D limit is already reached at $L_z = 190$ Å. It should be emphasized that even $L_z = 100$ Å samples, which are usually used for the investigation of 2D systems are—at least with respect to the screening properties—far away from the strict 2D limit.

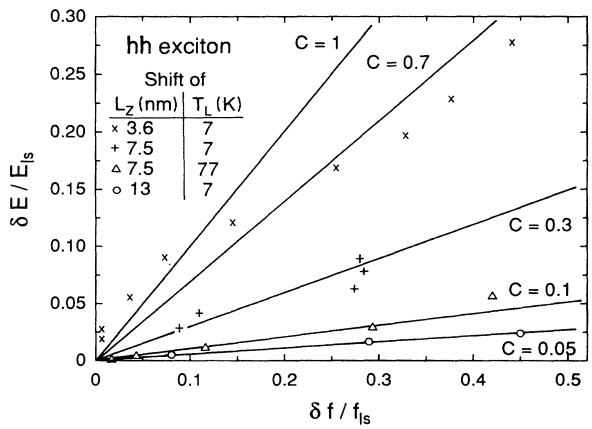

FIG. 3. Shift of the 1hh-x as a function of its decreasing oscillator strength.

IV. HIGH-DENSITY REGIME: THE ELECTRON-HOLE PLASMA

It was another aim to determine the plasma density N_c and the renormalized band gap E_g' by evaluating the gain

and luminescence spectra. In the following considerations we assume for simplicity parabolic subband structures for electrons and holes to make use of the effective-mass approximation.

To obtain the plasma temperature directly from the luminescence spectra $L(\hbar\omega)$ one can use[19]

$$L(\hbar\omega) \propto \exp\left[-\frac{\hbar\omega}{k_B T_{\text{eff}}}\right] \quad \text{for } \hbar\omega-\mu \gg k_B T_{\text{eff}} \tag{6}$$

with

$$\frac{1}{T_{\text{eff}}}=\frac{m_h}{m_e+m_h}\frac{1}{T_e}+\frac{m_e}{m_e+m_h}\frac{1}{T_h} \tag{7}$$

and $m_{e,h}$ and $T_{e,h}$ for the effective masses and temperatures of electrons (e) and holes (h), respectively; μ, the chemical potential of the created plasma.

Under quasistationary conditions we can assume that both electrons and holes have enough time to interact and reach the same temperature. Therefore we can write $T_{\text{eff}}=T_e=T_h$. The plasma densities N,P and the quasichemical potentials $\mu_{e,h}$ of electrons and holes are combined via

$$\left.\begin{matrix} N \\ P \end{matrix}\right\} = \sum_i \int D_{e,h}^{\text{2D}}(E) f_{e,h}(\mu_{e,h},E)\,dE \ . \tag{8}$$

$D_{e,h}^{\text{2D}}$ are the two-dimensional densities of states and $f_{e,h}$ the quasi-Fermi functions. To account for fluctuations of the well widths and for alloy disorder in the (Al,Ga)As barriers we replace the steplike density for band i by[20]

$$D_{e,h}^{\text{2D}}(E)=\frac{m_{e,h}}{\pi\hbar^2}\frac{1}{1+\exp\left[\dfrac{E-E_{g,i}}{\varepsilon}\right]} \ . \tag{9}$$

The adjustable parameter ε is to be fitted to the experimental data. Typical values which we used are $\varepsilon=1-2$ meV. If we use the constant density of states instead of Ref. 9, Eq. (8) leads to smaller values for N and P, respectively. The difference increases with decreasing temperature and μ (see Fig. 5).

With the assumption of momentum conservation for the optical transitions and of a constant matrix element and by neglecting the correlation enhancement due to the high carrier temperatures, the luminescence and gain spectra are given in the most simple case[21] by

$$\left.\begin{matrix} L(\hbar\omega) \\ G(\hbar\omega) \end{matrix}\right\} = \sum_{i,j}\alpha_{ij}\int_{-\infty}^{+\infty} D_e^{\text{2D}}(E,E_i)D_h^{\text{2D}}(E,E_j)F_{L,G}(E) \times \delta_\Gamma(\hbar\omega-E)\,dE \ . \tag{10}$$

Using a two-band system for the interaction of carriers with the electric field we obtain

$$F_L(E)=f_e(E)f_h(E) \tag{10a}$$

and

$$F_G(E)=1-[f_e(E)+f_h(E)] \tag{10b}$$

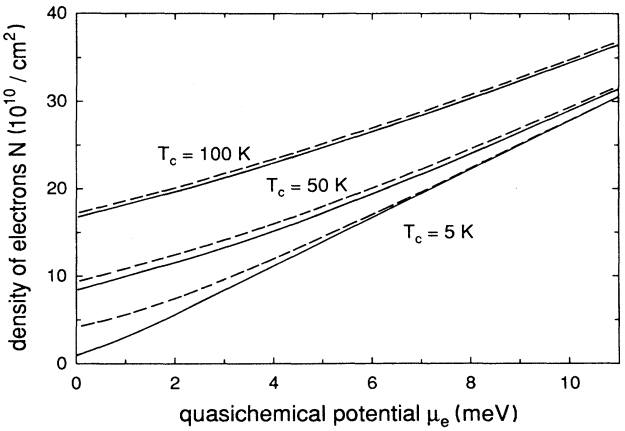

FIG. 5. Theoretical dependence of the quasichemical potential μ_e on the density of electrons n at various plasma temperatures T_c [solid (dashed) lines: model with steplike (broadened) density of states].

for the luminescence and absorption (gain) spectra, respectively.

The factor α_{ij} in Eq. (10) is equal to 1 for electron–heavy-hole (e-hh) and $\frac{1}{3}$ for electron–light-hole (e-lh) transitions, taking into account that the e-lh oscillator strength is roughly three times weaker than the e-hh one.[22,23] The sum has to be taken over all subbands i,j. We consider the limit of infinite barrier heights for the optically allowed transitions, where only terms with $i=j$ will remain. The contributions of terms with $i,j \geq 2$ are negligible for low carrier densities ($n_c < 8\times10^{11}$ cm^{-2}) as shown below. To calculate the subband energies E_i,E_j we assume rectangular potentials with finite barriers; the matching conditions across the (Al,Ga)As-GaAs interfaces are the continuities of the envelope function (Ψ) and of $m^{-1}d\Psi/dz$.[24] The deviations from the parabolic behavior of the lh and hh dispersion due to the breakdown of degeneracy of their energies at the Γ point and the noncrossing rule[25] are completely neglected. The effective masses used in our fits were $m_e=(0.067+0.084x)m_0$, $m_{\text{lh}}=(0.087+0.063x)m_0$, and $m_{\text{hh}}=(0.48+0.31x)m_0$ in the $Al_xGa_{1-x}As$ barriers[26] and we have chosen, for the quantum well, values $m_e=0.067m_0$,[26] $m_{\text{lh}}=0.094m_0$, $m_{\text{hh}}=0.34m_0$;[27] herein m_0 denotes the mass of the free electron. For the values of the band offsets of valence and conduction band V_v and V_c, we assumed $V_c=0.62(1.247x)$ eV (Ref. 25) and $V_c/V_v=62/38$.[28] The expression $\delta_\Gamma(\hbar\omega-E)$ replaces a δ function which expresses the conservation of energy in (10). δ_Γ takes into account the final-state damping of the photocreated carriers[29,30] and is defined as

$$\delta_\Gamma(x)\frac{1}{\pi}\frac{\Gamma}{x^2+\Gamma^2} \ . \tag{11}$$

The full width at half maximum (FWHM) Γ of this Lorentzian profile is chosen as a function of the energy E with its maximum $\Delta+\Gamma_0$ at the band gap $E_{i,j}$ and a value decreasing towards the chemical potential $\mu=\mu_e+\mu_h$,[29]

$$\Gamma=\Gamma(E)\begin{cases}\dfrac{\Gamma_0-\Delta}{E_{i,j}-\mu}(E-\mu)+\Delta & \text{if } E\le\mu\\ \Delta & \text{otherwise}\end{cases} \tag{12}$$

with $\Delta \ll 1$ meV. Typical values for the parameter Γ_0 are 2–3 meV. In Refs. 31 and 32 an increasing Γ is assumed for $E>\mu$. Recent publications on 2D systems[32] show that a fit with this model leads to lower plasma temperatures. A check which we made to compare both models gave plasma temperatures not more than 20% smaller than those using Eq. (12).

The assumptions and approximations made in this model are good enough to achieve a nice agreement with our measurements. We were able to evaluate experimental data over more than two orders of magnitude of the exciting optical power flux density $I_{\rm exc}$ (≤ 1 up to 420 kW/cm^2) with resulting plasma densities N_c between 10^{11} and 10^{12} cm^{-2}. The limitations of this concept are the transition to the density regime dominated by excitons at low densities and the increase of stimulated emission preferentially in the plane of the platelet samples at high densities. Figure 6 shows some results concerning the MDQW for a lattice temperature $T_L=77$ K. The calculated reduced fundamental band gap is marked by an arrow. It is satisfactory to see that the low-energy structure in Fig. 6(b) which we ascribe to the onset of stimulated emission at the Γ point takes place at the same energy. The difference of both theory and experiment at the high-energy tail of this spectrum is due to the population of and subsequent transitions from the second subband, which were neglected in the calculations.

Our results show significant deviations from those of Bogiovanni, Staehli, and Martin,[33] and of Tränkle *et al.*,[34] respectively. The first group gets values for the shift of E_g' which are about 5 meV too low in comparison with our results, but are in accordance with ours if we use a constant density of states in our calculations. The results of Tränkle *et al.* for the shift are about 10–15 meV too high; the reasons for the deviations have been already briefly discussed in Ref. 33.

If the incoming light power density is high enough to create a degenerate *e-h* plasma, it is possible to deduce the plasma parameters by detecting the optical gain.[35–37] The values for E_g' and μ are determined roughly by the extreme points of the observed gain spectrum, i.e., by the region of negative absorption coefficient. Two examples are given in Fig. 7. The way how the densities are deduced from the gain spectra is given in Ref. 35. The comparison of both methods, luminescence, and gain spectroscopy shown in Fig. 8 for the MDQW sample gives an excellent agreement. The dashed calculated line represents a result of a dynamical single plasmon-pole approximation;[38] to make the calculation comparable to the experimental data of a MDQW, we assumed for the reduced band gap

$$E_g'=E_g'(N_D)+\tfrac{1}{2}A\,[N_D^{1/3}-(N^{1/3}+P^{1/3})] \tag{13}$$

with $N=N_{\rm exc}+N_D$, where N_D is the electron density in the well due to modulation doping and $N_{\rm exc}$ the addition-

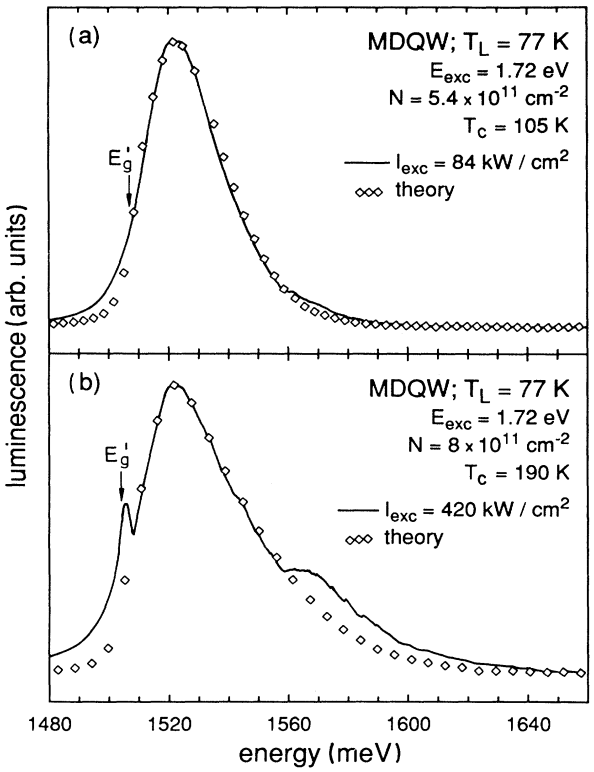

FIG. 6. Line-shape analysis of the MDQW luminescence at a lattice temperature of $T_L=77$ K with $I_{\rm exc}=84$ kW/cm^2 (a) and 420 kW/cm^2 (b).

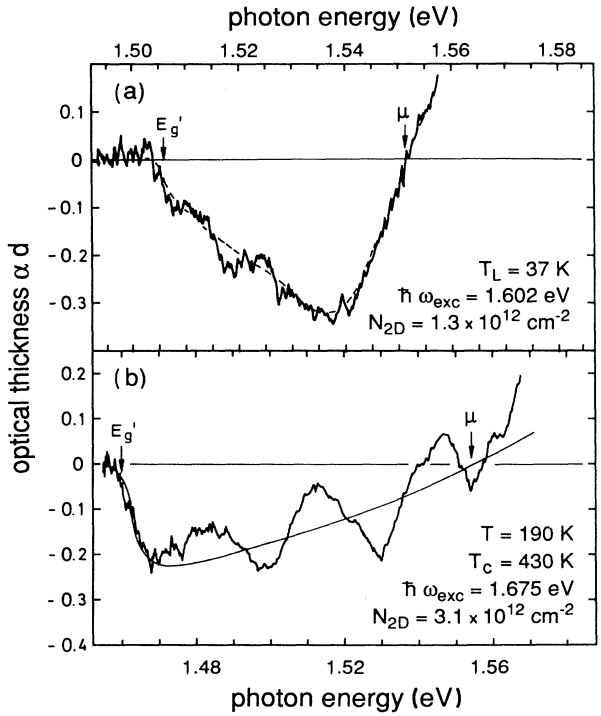

FIG. 7. Gain spectra of a 50×130 Å MQWS at various lattice temperatures.

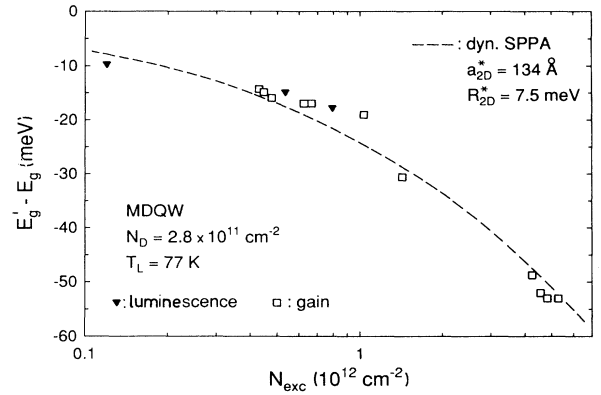

FIG. 8. Comparison of the results for the band-gap renormalization from luminescence and gain data with a dynamical single-plasmon-pole approximation (dynamical SPPA).

al one caused by photoexcitation; A is to be fitted to the experimental data.

Equation (13) makes use of the assumption that each subband shift depends only on the number but not on the types of carriers. Previous calculations of the renormalization of a one-component plasma[39] show that electron and hole subbands shift by a fairly equal amount and almost half as far as in the common two-component case.

Recent publications and research activities[40,41] about MDQW structures with $N_D > N_s$ were able to ascribe an observed low energetic structure to the correlation enhancement around the spectral position of the chemical potential. It is shown in this contribution that this phenomena reveals characteristics in the pump and probe spectra which are different from those of excitonic bleaching mechanisms.

Figure 9 shows absorption spectra of a 149-Å MDQW at $T_L = 10$ K. The spectra lead from $N_{exc} = 0$ (top line) to $N_{exc} = 2.4 \times 10^{11}$ cm^{-2} (lowest line) of optically created carriers. Although we excited only slightly above the absorption edge to prevent carrier heating, carrier temperatures of about 95 K were reached in the last case. The effects of the increasing carrier density are a reduction of height and a blue shift of the structure. The observed shift is in contradiction to the excitonic bleaching of comparable undoped samples where the spectral position is nearly fixed, but can be explained by a shift to higher energies of the absorption edge due to the filling of the continuum states. The reduction of the absorption height is in accordance with theoretical results[38,40,41] where the breakdown of the correlation enhancement with increasing density and temperature is predicted. It should be finally pointed out that the light power density needed to bleach the MDQW structure in Fig. 9 is about 5 kW cm^{-2} while we found out that 130 W cm^{-2} are enough for the 1hh-x resonance of a 130-Å MQW at $T_L = 7$ K. This means that the necessary light power is a good criterion to decide between both effects.

V. RENORMALIZATION OF HIGHER SUBBANDS

Concerning the investigation of the renormalization of the higher subbands (RHS) with $n_z \geq 2$ two limiting cases can be distinguished.

(i) At low light power densities the excitonic effects dominate the absorption spectra. The higher subbands are not occupied by carriers and therefore are only influenced by intersubband interactions with the carriers in the lowest subbands.

(ii) Increasing pump power leads to an occupation of the $n_z \geq 2$ subbands; for that reason bandfilling effects become important for the RHS.

At excitation levels between these limiting cases one can get additional information about the bleaching mechanisms of the higher-subband excitons.

To achieve the shifts of the higher subbands ΔE_i, $i \geq 2$ in the first case, we assumed constant exciton binding en-

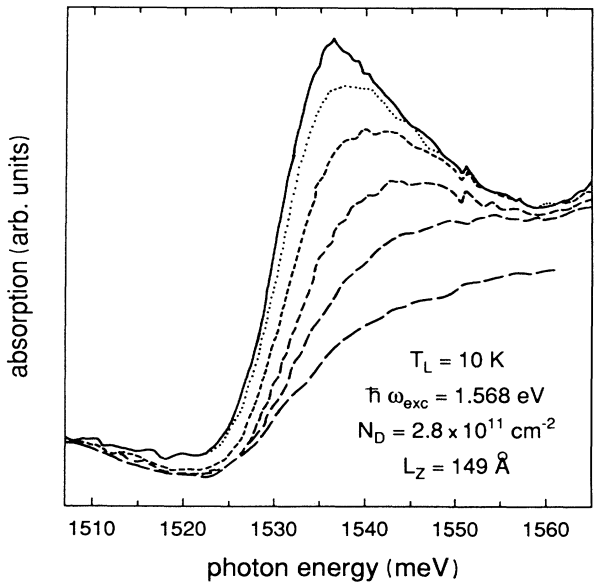

FIG. 9. Decrease of the correlation enhancement and bleaching of the absorption edge of a MDQW with increasing excitation density.

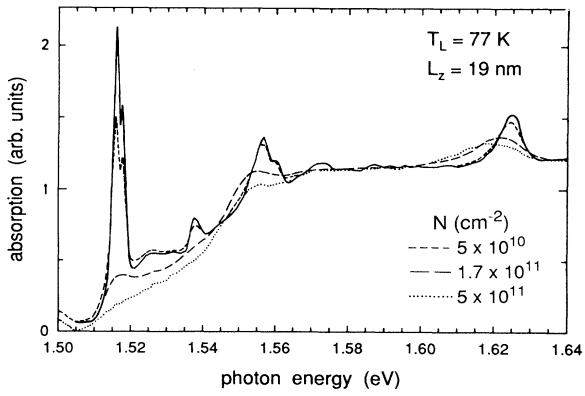

FIG. 10. Absorption spectra of a 190-Å MQWS at $T_L = 77$ K and $E_{exc} = 1.675$ eV. The carrier densities are 5×10^{10} (— — —), 1.7×10^{11} (---), and 5×10^{11} cm^{-2} (. . . .).

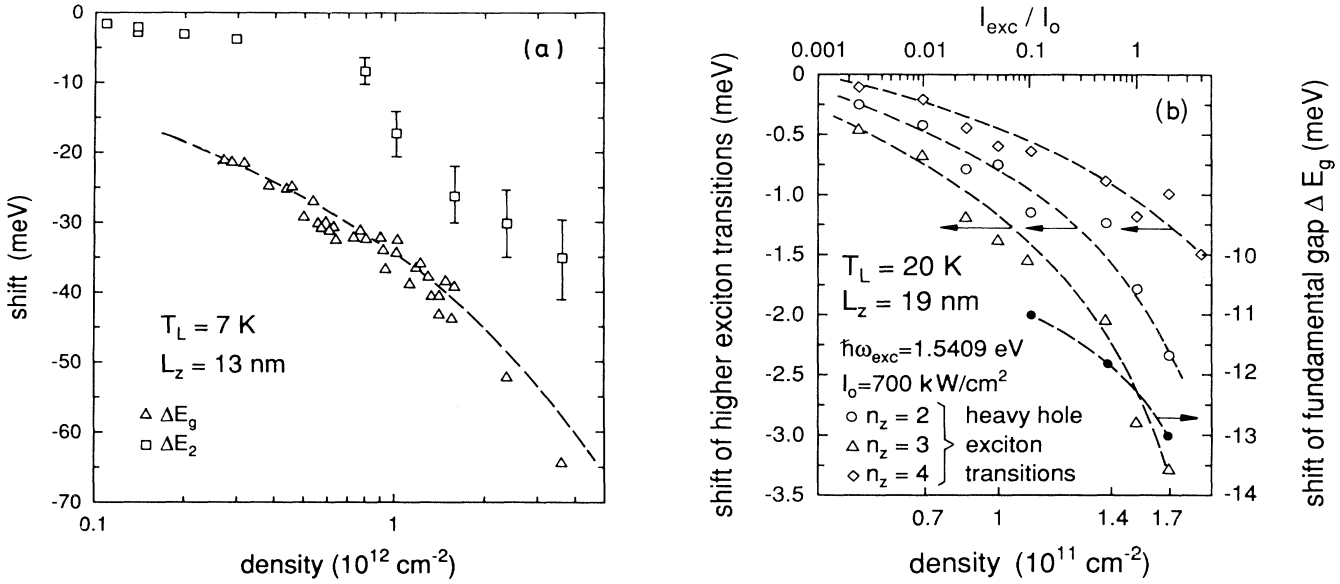

FIG. 11. (a) Shift of the fundamental band gap ΔE_g and of the second subband ΔE_2 for a 130-Å MQWS. The curve represents a 2D theory with effective parameters (Ref. 38). (b) Shift of the fundamental band gap and comparison between the shifts of the 2hh, 3hh, and 4hh excitons for a 190-Å MQW. The excitation energy $\hbar\omega_{exc}$ was slightly above the 1hh-x.

ergies $E_{1s,i}$. This simplification leads to an underrating of the estimated subband shifts, but we assume the discrepancy to be small as long as the excitonic resonance of that subband is clearly observable.

Figure 10 shows pump- and probe-beam measurements on a 30×190 Å MQWS. The 1hh-x and 1lh-x are located around $E=1.52$ eV, the 2hh-x at 1.56 eV, and the 3hh-x at 1.625 eV. To determine the carrier density N_c for small pump intensities we evaluate the 1hh-x oscillator strength. Values above the exciton bleaching density are obtained from absorption line-shape analysis.[42,43] With increasing N_c we observe the bleaching of the $n_z=1$ excitons due to direct occupation. After that the 2hh-x structure vanishes. The 3hh-x shows only a slight red shift. A line-shape analysis with a Lorentzian shape reveals that the area under the absorption peak remains almost constant. Within this model the broadening and the reduction of the peak height are due to scattering processes with carriers of the lower subbands. A rough estimation of the carrier densities in the various populated subbands leads to the following result: the exciton bleaching of the higher subbands is mainly due to phase-space filling and exchange interactions, which are pure population effects. The exciton ionization via the intersubband screening is practically negligible.

In Fig. 11(a) the band-gap shift for the $n_z=1,2$ transitions of a 50×130 Å MQWS are given. It is clearly recognizable that in the region of unpopulated higher subbands with densities below 8×10^{11} cm^{-2} (Ref. 44) only a slight shift ΔE_2 can be observed. As soon as the occupation of the $n_z=2$ subband sets in, a drastic decrease of the subband edge starts. Most recent theoretical results[45] are in good accordance with the observed behavior. The shift is in the order of magnitude which one would estimate from the direct occupation density of the $n_z=2$ subbands. This result fits well with the observation of the independently shifting subbands of the MDQW. Hence the interaction of carriers in different subbands—irrespective of their type of charge—appears to be very weak. Figure 11(b) shows similar results for a wider MQW sample. Again the shift of the higher subbands is small compared to the shift of the fundamental gap as long as the higher subbands are not populated.

ACKNOWLEDGMENTS

This work has been supported by the Deutsche Forschungsgemeinschaft and by the Materialforschungsschwerpunkt des Landes Rheinland-Pfalz. Stimulating discussions with H. Haug, C. Ell, H. Kalt, and W. W. Rühle are acknowledged.

[1]IEEE J. Quantum Electron. **QE-22**, 9 (1986) (Special Issue on Semiconductor Quantum Wells and Superlattices: Physics and Applications, edited by D. S. Chemla and A. Pinczuk).

[2]IEEE J. Quantum Electron. **24**, 9 (1988) (Special Issue on Semiconductor Quantum Well Heterostructures and Superlattices, edited by J. J. Coleman).

[3]*Optical Switching in Low-Dimensional Systems*, Vol. 194 of *NATO Advanced Study Institute, Series B: Physics*, edited by H. Haug and L. Banyai (Plenum, New York, 1989).

[4]J. J. LePore, J. Appl. Phys. **51**, 6441 (1980).

[5]S. Schmitt-Rink, D. S. Chemla, and D. A. B. Miller, Phys. Rev. B **32**, 6601 (1985).

[6]R. Zimmermann, Phys. Status Solidi B **146**, 371 (1988).
[7]H. C. Lee, A. Kost, M. Kawase, A. Hariz, P. D. Dapkus, and E. Garmire, IEEE J. Quantum. Electron. **QE-24**, 1581 (1988).
[8]S. H. Park, J. F. Morhage, A. D. Jeffrey, R. A. Morgan, A. Chavez-Pirson, H. M. Gibbs, S. W. Koch, N. Peyghambarian, M. Derstine, A. C. Gossard, J. H. English, and W. Weigmann, Appl. Phys. Lett. **52**, 1201 (1988).
[9]D. Hulin, A. Mysyrowicz, A. Antonetti, A. Mingus, W. T. Masselink, H. Morkoc, H. M. Gibbs, and N. Peyghambarian, Phys. Rev. B **33**, 4389 (1986).
[10]G. W. Fehrenbach, W. Schäfer, J. Treusch, and R. G. Ulbrich, Phys. Rev. Lett. **49**, 1281 (1982).
[11]F. A. Majumder, H.-E. Swoboda, K. Kempf, and C. Klingshirn, Phys. Rev. B **32**, 2407 (1985).
[12]H.-E. Swoboda, F. A. Majumder, V. G. Lyssenko, G. Klingshirn, and L. Banyai, Z. Phys. B **70**, 341 (1988).
[13]E. Lach, G. Lehr, A. Forchel, K. Ploog, and G. Weimann, *Proceedings of the International Conference on the Physics of Semiconductor Structures, Ann Arbor, MI, 1989* (North-Holland, Amsterdam, 1990); Surf. Sci. **228** (1990).
[14]S. Schmitt-Rink, D. S. Chemla, D. A. B. Miller, Adv. Phys. **38**, 89 (1989).
[15]D. Huang, H. Y. Chu, Y. C. Chang, R. Houdre, and H. Morkoc, Phys. Rev. B **38**, 1246 (1988).
[16]Y.-C. Chang, and G. D. Sanders, Phys. Rev. B **32**, 5521 (1985).
[17]P. Nozières and C. Comte, J. Phys. (Paris) **43**, 1083 (1982).
[18]W. Schäfer, R. Binder, H.-H. Schuldt, and J. Treusch, *Proceedings of the 18th International Conference on the Physics of Semiconductors, Stockholm, 1986* (World Scientific, Singapore, 1987).
[19]J. Shah, IEEE J. Quantum. Electron. **QE-22**, 1728 (1986).
[20]D. S. Chemia, D. A. B. Miller, P. W. Smith, A. C. Gossard, and W. Wiegmann, IEEE J. Quantum Electron. **QE-20**, 265 (1984).
[21]R. N. Hall, Solid State Electron. **6**, 405 (1963).
[22]P. Voisin, G. Bastard, and M. Voos, Phys. Rev. B **29**, 935 (1984).
[23]W. T. Masselink, P. J. Pearah, J. Klem, C. K. Peng, and M. Morkoç, Phys. Rev. B **32**, 8027 (1985).
[24]I. Gailbraith and G. Duncan, Phys. Rev. B **38**, 10057 (1988).
[25]G. Bastard and J. A. Brum, IEEE J. Quantum Electron. **QE-22**, 1625 (1986).
[26]N. Watanabe and H. Kawai, J. Appl. Phys. **60**, 3696 (1986).
[27]D. S. Chemla (private communication).
[28]E. O. Göbel (private communication).
[29]P. T. Landsberg, Phys. Status Solidi **15**, 623 (1966).
[30]P. T. Landsberg, Solid State Electron. **28**, 137 (1985).
[31]C. Klingshirn and H. Haug, Phys. Rep. **70**, 5 (1981); **70**, 315 (1981).
[32]J. H. Collet, W. W. Rühle, M. Pugnet, K. Leo, and A. Million, Phys. Rev. B **40**, 12 296 (1989).
[33]G. Bongiovanni, J. L. Staehli, and D. Martin, Phys. Status Solidi B **150**, 685 (1988).
[34]G. Tränkle, H. Leier, A. Forchel, H. Haug, C. Ell, and G. Weimann, Phys. Rev. Lett. **58**, 419 (1987).
[35]Ch. Weber, C. Klingshirn, D. S. Chemla, D. A. B. Miller, J. Cunningham, and C. Ell, Phys. Rev. B **38**, 12 748 (1988).
[36]C. Klingshirn, Ch. Weber, D. S. Chemla, D. A. B. Miller, J. E. Cunningham, C. Ell, and H. Haug, in *Advanced Study Institute, Series B: Physics,* edited by H. Hang and L. Bányai (Plenum, New York, 1989), Vol. 194, p. 353.
[37]Ch. Weber, K.-H. Schlaad, D. Oberhauser, H. Kalt, C. Klingshirn, D. S. Chemla, J. Cunningham, G. Weimann, W. Schlapp, and H. Nickel, in *Proceedings of the Seventh International Conference on Dynamical Processes in Excited States of Solids, Athens, GA, 1989,* edited by R. S. Meltzer, J. E. Rives, and W. M. Yen (North-Holland, Amsterdam, 1990); J. Lumin. **45**, 201 (1990).
[38]S. Schmitt-Rink and C. Ell, J. Lumin. **30**, 585 (1985).
[39]C. Ell (private communication).
[40]M. Wegener (private communication).
[41]G. Livescu, D. A. B. Miller, D. S. Chemla, M. Ramaswamy, T. Y. Chang, N. Sauer, A. C. Gossard, and J. H. English, IEEE J. Quantum Electron. **QE-24**, 1677 (1988).
[42]C. Ell and H. Haug (unpublished).
[43]Ch. Weber, Ph.D. thesis, Fachbereich Physik der Universität Kaiserslautern, 1989.
[44]W. H. Knox, C. Hirlimann, D. A. B. Miller, J. Shah, D. S. Chemla, and C. V. Shank, Phys. Rev. Lett. **56**, 1191 (1986).
[45]C. Ell and H. Haug, Phys. Status Solidi B **159**, 117 (1990).